Section-Thickness Profiling for Brachytherapy Ultrasound Guidance

Mohammad Peikari[a], Thomas Kuiran Chen[a], Everette C. Burdette[b], Gabor Fichtinger[a]

[a]School of Computing, Queen's University, Kingston, Canada;
[b]Acoustic MedSystems Inc, Illinois, USA

ABSTRACT

Purpose: Ultrasound (US) elevation beamwidth causes a certain type of image artifact around the anechoic areas of the tissue. It is generally assumed that the US image is of zero thickness, which contradicts the fact that the acoustic beam can only be mechanically focused at a depth resulting in a finite, non-uniformed elevation beamwidth. We suspect that elevation beamwidth artifacts contribute to target reconstruction error in computer-assisted interventions. This paper introduces a method for characterization of the beamwidth for transrectal ultrasound (TRUS) used in prostate brachythyerapy. In particular, we measure how the US scetion-thickness varies along the beam's axial depth. Method: We developed a beam-profiling device (a *TRUS-bridge* phantom) specifically tailored for standard brachytherapy ultrasound imaging systems to generate a complete section-thickness profile of a given TRUS transducer. The device was designed in CAD software and prototyped by a 3D printer. Result: The experimental results demonstrated that the TRUS beam in the elevation direction is focused closely to the transducer and theoretically the transducer would provide a better elevational resolution within that range. Conclusion: We presented a beam profiling phantom to measure the section-thickness of a transrectal ultrasound transducer for operating room use. However, there are some limitations which need to be addressed, for example, phantom sterilization and the speed of sound in the current medium of experiment which is not the same as that of biological tissues.

Keywords: beamwidth, section-thickness, ultrasound imaging, brachytherapy.

1. INTRODUCTION

Ultrasound (US) is an attractive imaging modality because it is widely available, non-ionizing, and can visualize in real-time almost any body tissue. However, due to the physics of the US beam propagation through the medium and image formation, the acquired US images may contain a certain artifact along the beam's elevational axis. This artifact commonly appears in anechoic areas[1] that hiders the identification of tissue structures and the ability to make appropriate medical diagnoses.

1.1 The US Physics

The transducer in an US machine sends and receives the soundwaves. US soundwaves propagate through the medium when excitation pulses are applied to each element (crystal) of the array transducer. In A-mode scanning, an ultrasound beam is propagated from one (or a group) of crystal(s) on the transducer. The transducer is then "silent" for a small fraction of time, waiting for return echoes from the medium before it generates the next pulse; this process continues by exciting each set of crystals on the US transducer. The information from each line of sight (a line of sight represents activation of one or a group of crystals in the transducer array) is then put together to form an US B-mode image.

Focusing is a way to improve the resolution of an US B-mode image; the narrower the beam, the better the image quality. Focusing can be achived in two ways, *mechanically* and *electronically*[2] . In mechanical focusing,

Further author information: (Send correspondence to G. Fichtinger.)
M. Peikari: E-mail: mpeikari@cs.queensu.ca
T. K. Chen: Email: chent@cs.queensu.ca
E. C. Burdette: Email: clifb@acousticmed.com
G. Fichtinger: Email: gabor@cs.queensu.ca, Telephone: 1 613 533 6050

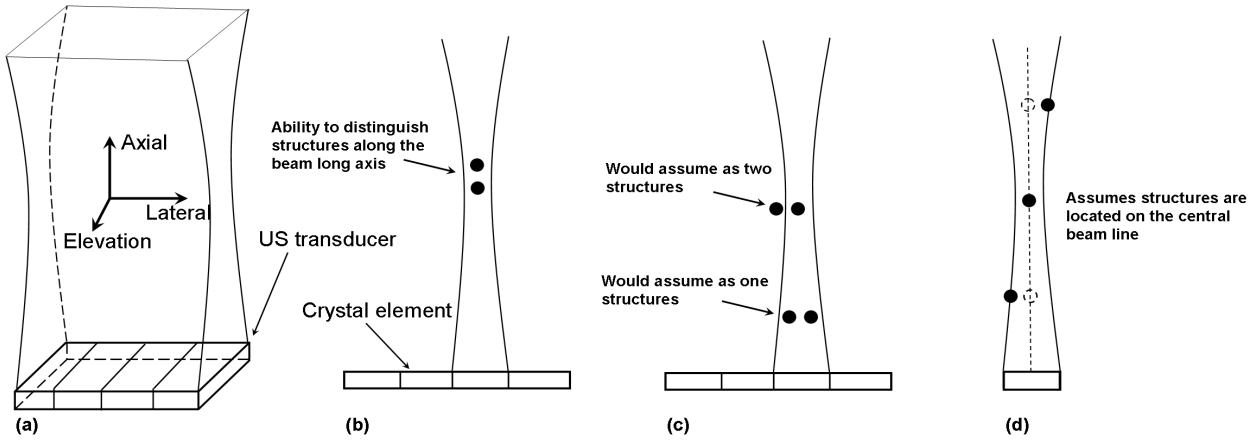

Figure 1. (a) US beam pattern in *Axial, Lateral,* and *Elevation* axes. (b) Axial resolution, (c) Lateral resolution, and (d) Elevation resolution.

US beams are passed through an acoustic lense which works in the same manner as an optical lense (external focusing), or by curving crystals which bends the soundwaves toward a point in the tissue (internal focusing). Mechanical focusing is typically employed to improve imaging resolution in the elevation direction[2] . Electrical focusing however, is a more sophisticated technique which is based on using timing circuits and clocks, and alternative sequences of firing various crystals in a group by a small time delay. Electrical focusing is typically used to narrow the US beam in the lateral direction[2] .

US image quality may be explained using three different factors: axial resolution (ability to distinguish between two reflecting points along the long axis of the beam), lateral resolution (ability to distinguish between two reflecting points perpendicular to the long axis of the beam), and elevation resolution (out-of-plane direction)[2] as depicted in Fig. 1. The effect of the section-thickness artifacts in the US elevation plane can be explained in detail using Fig. 2.

Figure 2(a) shows the cross section of an unfocused beam pattern when it leaves a linear array transducer crystal. Figure 2(b) shows the A-mode echoes received by the transducer in presence of a reflecting material (human tissue). The first three reflected beams correspond to the three objects in the near-field located at the same depth (time) to the front end of the transducer. Since the strength of an US beam is highest at its center and decreases gradually toward the side edges[1] , the maximum reflection intensity corresponds to point A which is located along the axial path of the beam. Reflection levels corresponding to points B and C are lower because they are close to the side edge of the beam pattern.

Points D-F are located farther from the US beam and their reflection intensities follow the same concept, with the exception that, the overall intensity of the US beam decreases as it propagates through the medium. Hence point D has the highest reflection intensity and point F the least. The echoes reflected from objects at a known depth along the axial path and lateral position of the US beam will be absorbed simultaneously. The transducer sums all the echo reflections at a time and interprets its value as a single reflecting object located on the beam's central line[1] . This means, even if there is no reflecting object located on the central beam ray, the device assumes that the reflected echo corresponds to an object along the central portion of the beam pattern. This is depicted as point G in Fig. 2(b) and as an object tissue in Fig. 3 (a). The closer the reflecting object is to the central beam ray the less the section-thickness artifacts will be and vice versa[1] .

Inspired by Goldstein's original principle and its variants[1,3,4] , we have previously designed a *Bridge* phantom to measure the section-thickness for US freehand imaging and used the results to improve the calibration precision.[5] In this paper, we propose a practical and more precisely designed beamwidth profiling technology that is specifically tailored for the industry-standard brachytherapy transrectal US imaging.

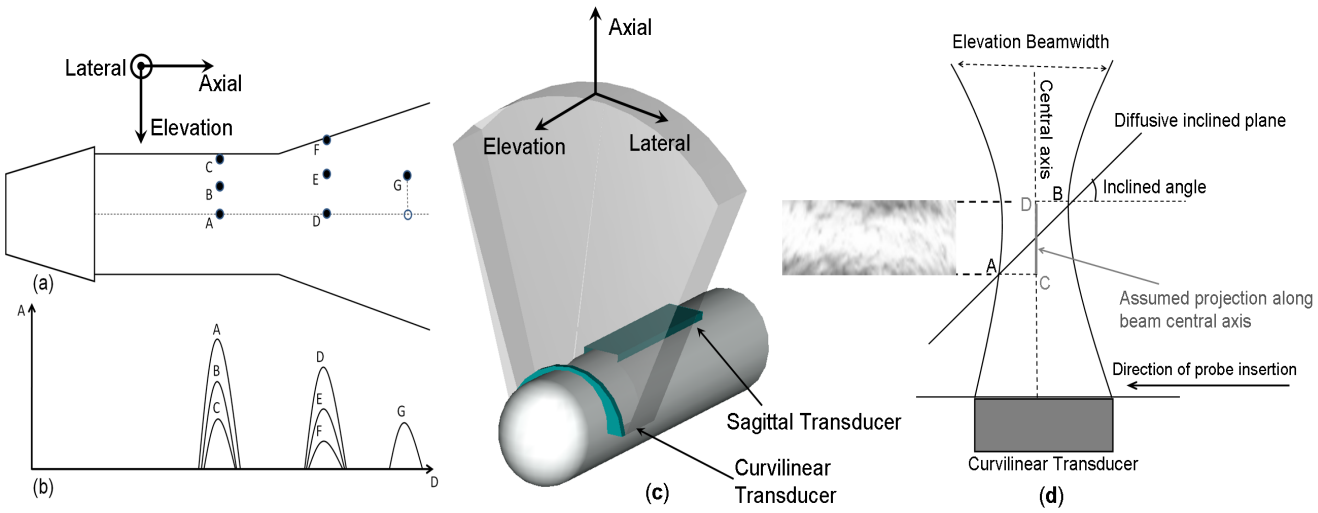

Figure 2. (a)-(b) Beam pattern of the B-mode and A-mode linear array US with corresponding point reflectors[1] . (c) Axial, lateral and elevational axes convention with respect to the TRUS beam pattern. (d) Section-thickness estimation principle.

1.2 Prior Art

Goldstein[1] observed the effects of the section-thickness on the US images by changing the angle of the inclined surface for various experiments. In his work, he was not concerned about measuring the thickness of the artifacts on the US images. Richard,[4] tried to measure the US section-thickness by using several inclined surfaces located successively below each other in a phantom to capture many section-thickness artifacts in a single image for low frequency probes. One challenge in his work was holding and maintaining the probe at a 45° angle during the experiments.

Skolnick[3] used both an inclined surface and a phantom with multiple filaments located 1cm apart in a vertical row. He compared both the scan plane and elevation plane section-thicknesses by sweeping the linear array US probe oriented 90° and 45° to the filaments respectively. He obtained very close results when comparing the elevational section-thickness at specified depth using both the phantoms. He overcame the difficulty of holding the probe at the right pose by using a wooden jig.

1.3 The Clinical Brachytherapy Setup

In a brachytherapy procedure (Fig. 3(c)), the TRUS device is inserted into the patient's rectum for imaging the prostate. Radioactive seeds are placed within sharp hollow needles, which are inserted into the prostate through the perineum one at a time. The position coordiates within the prostate are reported using real-time ultrasound-guided visualisation of the needle as it advances through the prostate. During the procedure, needle tips are visible as a bright spot within the black prostate tissue in the TRUS images. Needles are inserted at a preplanned position through the patient's perineum with the help of the grid mounted on the TRUS stepper. Needle tips are manually tracked by the surgeon as they advance through the prostate in TRUS images and when they appear at a preplanned position, radioactive seeds are deposited in the prostate.

There are three important parts of a TRUS system to consider: a transrectal ultrasound probe, a stepper, and a grid template as shown in Fig. 3(b). The TRUS probe can move in and out of the patient's rectum allowing the brachytherapist to observe the prostate in live TRUS imagery during the procedure. The grid template located on the TRUS stepper guides the physician during the needle insertion process. The precisely machined stepper ensures that the TRUS probe always moves perpendicular to the grid template, and acquires TRUS images parallel to it.

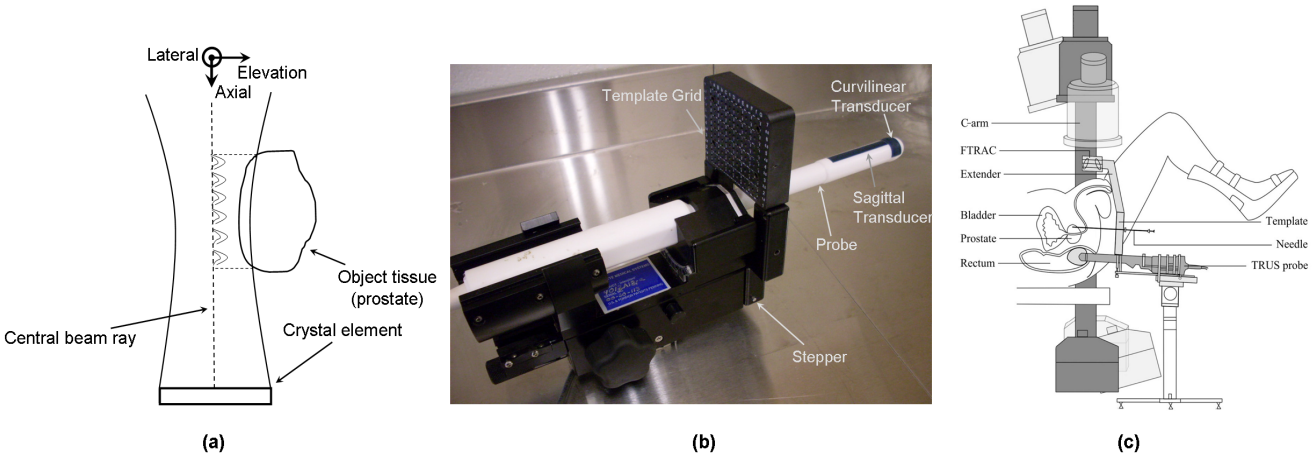

Figure 3. (a) Location of an object tissue (prostate) could be wrongly detected in presence of the US section-thickness[1] . (b) Different parts of the clinical TRUS device. (c) A schematic showing prostate brachytherapy procedure.

We modelled the US section-thickness, as the first step toward eliminating its effects on the TRUS images. Using the current TRUS stepper design as a frame work, we developed a simple phantom to estimate the ultrasound beam section-thickness.

2. METHODOLOGY

2.1 The Concept

We measured the section-thickness of the curvilinear transducer of a TRUS probe quantitatively using the approach described by Goldstein[1] . Figure 2(d) shows a cross-section of the beam pattern propagated from the TRUS curvilinear transducer intersected with an inclined diffusive material at 45° angle to the beam's central axis. Consider the diffusive material AB located at a known distance from the TRUS transducer. As the sound propagates through the medium, it first intersects point A and the transducer would receive an echo wave sooner than any other point along the beam's path. The last echo would be generated by point B which is located at the farthest distance from the transducer. However, the TRUS machine assumes all the received echoes are from the reflectors located at the central beam ray. Therefore, the reflection of the diffusive line AB would be represented as line CD located on the central beam ray. As a result, the TRUS image would include a thick bright band with its height equal to the length of CD. Furthermore, since the diffusive material makes a 45° angle to the central beam axis, the length of CD is approximately equal to the TRUS elevation beamwidth as shown in Fig. 2(d).

We designed the *TRUS-bridge* phantom such that the inclined plane makes a 45° angle to the vertical beam plane (Fig. 4(d)). The phantom was specifically designed to adapt on a standard brachytherapy system making use of the precisely machined encoded stepper. The phantom was equipped with stepper hole rods and side walls to prevent unwanted shakes and provide sufficient strength. The inclined surface of the phantom was made sufficiently long to show beamwidth artifacts in the TRUS images from all depths from the diffusive material. The phantom base also ensure that the diffusive surface always maintains its 45° angle to the probe. The supports to the inclined surface of the phantom eliminate the possibility of the diffusive surface bending, as shown in Fig. 4(a).

The TRUS beamwidth artifacts were segmeneted manually by choosing a few points from the boundary of the bright band on the TRUS images. The selected points were chosen from the central region of the beamwidth so as to ensure distorted parts of the bright band on the image sides are not influencing the true beamwidth measurements (in curvilinear arrays, the lateral resolution can occur when the scan line density reduces at depth[2]). The images were analyzed using a 2.33GHz Intel Core 2 Quad processor personal computer having a 3.25GB of RAM.

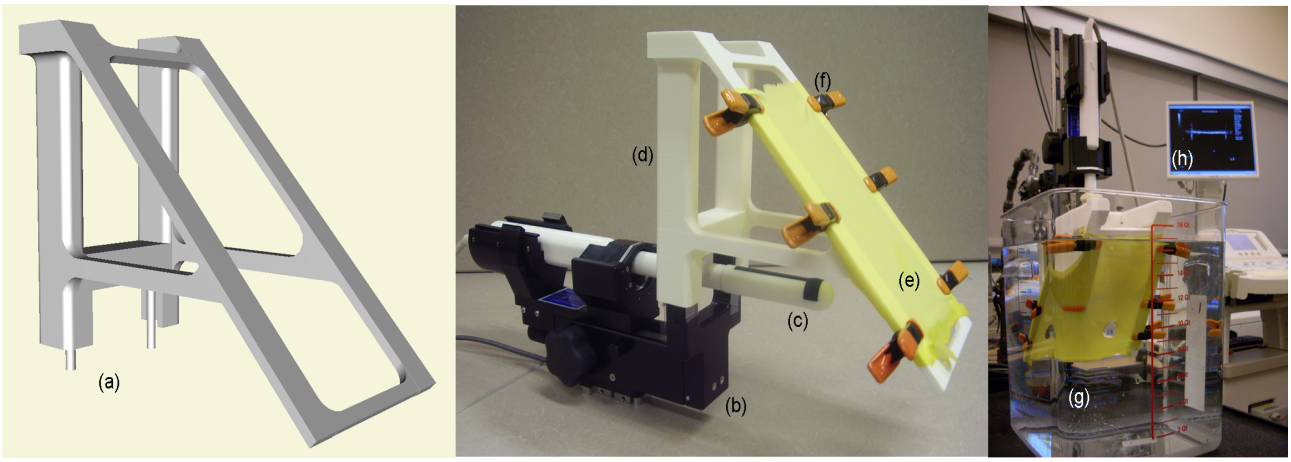

Figure 4. (a) CAD design of the *TRUS-bridge* phantom. (b) stepper, (c) transrectal probe, (d) *TRUS-bridge* phantom mounted on an industry-standard stepper, (e) rubber membrane on the inclined surface, (f) metal clamps, and (g)-(h) the experimental setup.

2.2 The Experimental Setup

To validate our design, we tested our phantom on a commercial grade probe stepper (Fig. 4(b)) (Burdette Medical Systems, IL, USA) but the design can be easily adapted to any other stepper.

The template grid was replaced by the *TRUS-bridge* phantom as shown in Fig. 4. A rubber membrane was used as a diffusive material (Fig. 4(e)) since its acoustic impedance is similar to that of water, making it a suitable sound reflector in water. The rubber membrane was held to the phantom using several rigid metal clamps (Fig. 4(f)), however, we aim to eliminate these in a future design. .

The TRUS probe (Fig. 4(c)) can move back and forth to capture the returning echos reflected by the diffusive surface. The distance from the TRUS transducer and the diffusive surface defines the depth at which the beamwidth is measured.

The precisely machined TRUS stepper (Fig. 4(b)) holds the phantom in the right pose so that the inclined surface remains at a 45° angle to the diffusive surface.

TRUS images were acquired at various depths when the whole system was inserted into a clear water bath as shown in Fig. 4(g). Images were acquired using the two available TRUS frequencies of 5MHz and 6MHz, as these are the frequencies normally used to observe the prostate during the brachytherapy procedures.

3. RESULTS

Using the *TRUS-bridge* phantom, we measured the elevation beamwidth at 29 different axial depths from the TRUS transducer. Fig. 5(a-b) illustrates a few examples of these measurements over various depths of the effective imaging region. The overall calculated beam profiles for the two operating frequencies are compared in Fig. 6. The measurements cover the axial depths from 27mm to 75mm from the TRUS transducer.

The beam in the elevation direction was focused closely to the transducer, i.e. the near-field of the US beam was relatively smaller than its far-field, e.g., at 5MHz the section-thickness starts with 3.16mm at 28.23mm axial depth and drops rapidly to 2.28mm at 29.13mm. Similarly at 6MHz the section-thickness starts with 3.04mm at 27.19mm axial distance and decreases to 2.59mm at 29.03mm axial distance from the TRUS transducer. This also indicates that the focal zone (around 29mm) corresponding to both the frequencies is located around the same axial depth. The beamwidth then starts diverging quickly after the focal zone to 6.08mm at 70.44mm and 6.71mm at 72.23mm for 5MHz and 6MHz frequencies respectively.

The overall pattern of the beam profile for both the frequencies tends to follow the same shape and remains within a limited boundary since the two operating frequencies were chosen to be close to each other. Table 1

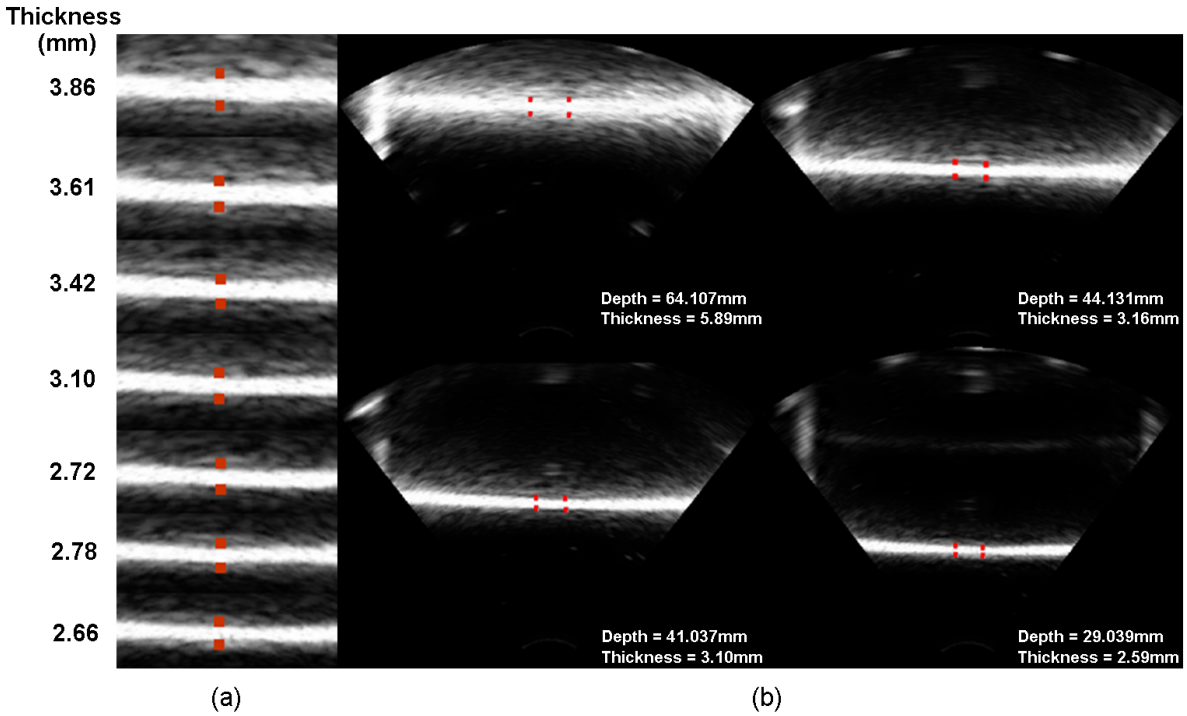

Figure 5. (a) A subset of elevation beamwidth measurements. (b) Examples of section-thickness artifacts over different depths of the TRUS images, frequency= 6MHz.

compares our results with previous experiments and shows that the focal length of different types of US probes may vary.

4. DISCUSSION

The fact that the focal zone is located close to its transducer essentially means that the TRUS device would provide a better elevational resolution within the focused beam region of the transducer.

The beamwidth segmentation procedure was manual and time-consuming however, the beam profile curve could have been smoother if the beamwidth segmentation procedure was performed automatically over several hundred acquired TRUS images.

We found that the TRUS device settings have direct impacts on the visibility of the section-thickness artifacts in the TRUS images. The thickness of the rubber membrane is negligible and hence the bright artifacts on the TRUS images are mainly due to the US section-thickness; for that reason, if the TRUS device settings (dynamic range, gain, and sector) are wrongly set, the correct boundary of the bright artifacts will not be visible in the TRUS images.

There is no sharp focal zone narrowing in the beam profile in the elevation plane. This could be due to the size of the curvilinear array (around 38mm) and its aperture (around 8mm).

Modifying the number of electronically set focal zones or the focal lengths in the image plane had no influence on the beam profile pattern. Focusing along the lateral axis of the image plane can only improve the quality of image formation (this observation is expected since the focusing along the elevation plane is achieved mechanically).

In addition, the estimated beam profile represents a localization error map in the acquired images. Incorporating this error map into the brachytherapy applications might give them the ability to consider the likelihood of

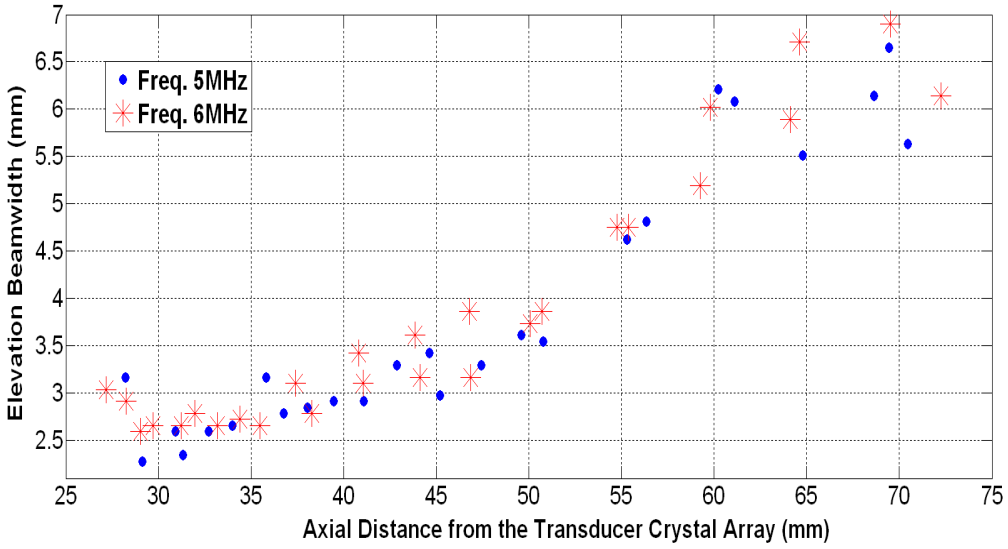

Figure 6. TRUS elevation beam profiles at 5MHz and 6MHz central operating frequencies.

position errors on the TRUS data which are otherwise treated uniformly in current practice. For example, according to the beam profiles, one should trust image regions near the elevation focal zone more than regions located at the greater depth where the localization uncertainty increases significantly with the growing section-thickness.

An advantage of our design was using the TRUS stepper as a support to ensure that the US beam plane displacement maintains exactly a 45° angle through out the experiment. This eliminated all the challenges in maintaining the soundwaves at a 45° angle to the inclined diffusive surface. The inclined surface supports also increase the reliability of the inclined surface to maintain the 45° angle during every step of the experiment.

The jigged beam profile points (mainly after 40mm axial depth) are probably due to error in manual segmentation, bad image resolution where the correct boundary of the beamwidth artifacts are not clear, or the effects of the mechanical play of the device.

Finally, our design is made to work with water as an imaging medium which differs from the speed of sound in the biological tissue (1540 m/s). Although this difference causes small measurement errors, more accurate results could be achieved by using a tissue-mimicing medium (e.g. Gel) in which speed and absorbtion of sound are similar to those in biological tissues.

5. FUTURE WORK

As future work, we plan to modify our *TRUS-bridge* phantom to be able to estimate the section-thickness of the TRUS curvilinear and sagittal transducers in successive experiments. Automating the process of beamwidth segmentation from a set of US images would help in finding a smoother beam profile curve from a few hundred US images. We plan to incorporate the estimated TRUS beam profiles (sagittal and curvilinear arrays) to improve the TRUS calibration accuracy.

We also suspect that the non-uniform beam pattern in the elevation direction may have negative impacts on the target localization error (TRE) in ultrasound-guided surgery applications. In future work, we plan to investigate the relationship of the TRE and the beam profile.

Author	Probe Type	Probe Central Frequency (MHz)	Elevation Focal Depth (mm)
Goldstein[1]	Linear array (long internal focusing)	3.5	Qualitative evaluation
	Linear array (short internal focusing)	3.5	No measurements reported
Richard[4]	Convex one-dimentional array	3.5	Qualitative evaluation
	Convex one and one-half-dimentional array	3.5	No measurements reported
Skolnick[3]	Phased array sector	3.5	60-80
	Curved array SP	7.5	20
	Curved array GP	7.5	40-60
Chen[5] *et.al*	Linear array	12.5	10.5
	Linear array	16	~ 12
Peikari *et.al*	TRUS	5	29.13
	TRUS	6	29.03

Table 1. Comparison summary of our results with previous experiments.

6. CONCLUSIONS

To the best of our knowledge there has been no previous work done to measure the TRUS beam profile. We presented the *TRUS-bridge* phantom to measure the section-thickness of a TRUS probe used in brachytherapy procedures. A set of TRUS images with the section-thickness artifacts was acquired using the phantom from various axial depths of the effective imaging region for the two available device frequencies. TRUS beamwidths were segmented manually by selecting a few points from the artifact's central portion to minimize the effects of distortion on the beamwidth measurment.

A beam profile of the segmented beamwidths were generated for all possible depths for the two central frequencies of 5MHz and 6MHz. In addition, we took the advantage of the precise design of the TRUS stepper as a frame work to ensure the TRUS beam ray always collides at a 45° angle to the diffusive surface.

ACKNOWLEDGMENTS

This work was funded by the Natural Sciences and Engineering Research Council of Canada under the Idea to Innovation program. Gabor Fichtinger was supported as Cancer Care Ontario Research Chair.

REFERENCES

1. A. Goldstein, B. M., "Slice thickness artifacts in gray-scale ultrasound," *J of Clin Ultrasound* **9**, 365–375 (Sep 1981).
2. F.W.Hedrick, D.L.Hykes, D., [*Ultrasound Physics and Instrumentation*], Elsevier Mosby, Missouri (2004).
3. Skolnick, M., "Estimation of beam width in the elevation (section thickness) plane," *Radiology* **108**, 286–288 (1991).
4. Richard, B., "Test object for measurement of section thickness at ultrasound," *Radiology* **211**, 279–282 (1999).
5. T.K.Chen, A.D.Thurston, M. R. P., "A real-time ultrasound calibration system with automatic accuracy control and incorporation of ultrasound section thickness," *SPIE Medical Imaging* (2008).